Accepted Manuscript

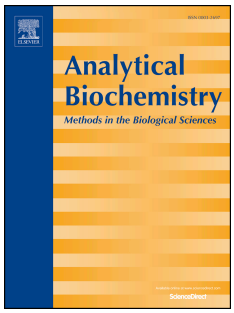

Fluorescence polarization-based assays for detecting compounds binding to inactive JNK3 and p38α MAP kinase

Francesco Ansideri, Andreas Lange, Ahmed El-Gokha, Frank M. Boeckler, Pierre Koch

PII: S0003-2697(16)00096-8

DOI: 10.1016/j.ab.2016.02.018

Reference: YABIO 12324

To appear in: *Analytical Biochemistry*

Received Date: 4 December 2015

Revised Date: 25 February 2016

Accepted Date: 26 February 2016

Please cite this article as: F. Ansideri, A. Lange, A. El-Gokha, F.M. Boeckler, P. Koch, Fluorescence polarization-based assays for detecting compounds binding to inactive JNK3 and p38α MAP kinase, *Analytical Biochemistry* (2016), doi: 10.1016/j.ab.2016.02.018.

Fluorescence polarization-based assays for detecting compounds binding to inactive JNK3 and p38α MAP kinase

Francesco Ansideri [a], Andreas Lange [b], Ahmed El-Gokha [a,c], Frank M. Boeckler [b], Pierre Koch[a]*

Address:

[a]Institute of Pharmaceutical Sciences, Department of Medicinal and Pharmaceutical Chemistry, Eberhard Karls Universität Tübingen, Auf der Morgenstelle 8, 72076 Tübingen, Germany

[b]Institute of Pharmaceutical Sciences, Molecular Design and Pharmaceutical Biophysics, Eberhard Karls Universität Tübingen, Auf der Morgenstelle 8, 72076 Tübingen, Germany

[c]Menofia University, Chemistry Department, Faculty of Science, Menofia, Egypt

*Corresponding author:

Email: Pierre Koch*- pierre.koch@uni-tuebingen.de

Keywords:

Fluorescence polarization; binding assay; c-Jun N-terminal kinase 3; p38α MAP kinase

[1]*Abbreviations used:* MAPK, mitogen-activated protein kinase; JNK, c-Jun N-terminal kinase; AD, Alzheimer's disease; PD, Parkinson's disease; ATP, adenosine triphosphate; HTS, high throughput screening; FP, fluorescence polarization; FITC, fluorescein isothiocyanate;

ELISA, enzyme-linked immunosorbent assay; MOE, molecular operating environment; rmsd, root-mean-square deviation; PDB, protein data bank; TLC, thin layer chromatography; HPLC, high performance liquid chromatography; DAD, diode array detector; NMR, nuclear magnetic resonance; ppm, parts per million; ESI-MS, electrospray ionization mass spectrometer; r.t., room temperature; BME, β-mercaptoethanol; BSA, bovine serum albumin; rpm, revolutions per minute; %CV, percent coefficient of variation; SD, standard deviation; ITC, isothermal titration calorimetry.

Abstract

Two fluorescein-labelled pyridinylimidazoles were synthesized and evaluated as probes for the binding affinity determination of potential kinase inhibitors to the c-Jun N-terminal kinase 3 (JNK3) and p38α mitogen-activated protein kinase (MAPK). Fluorescence polarization (FP)-based competition binding assays were developed for both enzymes using 1-(3',6'-dihydroxy-3-oxo-3*H*-spiro[isobenzofuran-1,9'-xanthen]-5-yl)-3-(4-((4-(4-(4-fluorophenyl)-2-(methylthio)-1*H*-imidazol-5-yl)pyridin-2-yl)amino)phenyl)thiourea (**5**) as an FP-probe (JNK3: K_d = 3.0 nM; p38α MAPK: K_d = 5.7 nM). The validation of the assays with known inhibitors of JNK3 and p38α MAPK revealed that both FP-assays correlate very well with inhibition data received by the activity assays. This, in addition to the viability of both FP-based binding assays for the high throughput screening procedure makes the assays suitable as inexpensive pre-screening protocols for JNK3 and p38α MAPK inhibitors.

1. Introduction

Within the mitogen-activated protein kinase (MAPK)[1] family, the two serine/threonine kinases c-Jun N-terminal kinase 3 (JNK3) and p38α MAPK have emerged in the last decades as particularly attractive therapeutic targets due to their implication in several pathologic conditions. JNK3, which is predominantly expressed in the brain, is associated with

neurodegenerative diseases such as Alzheimer's disease (AD), Parkinson's disease (PD) and Huntington's disease [1, 2]. On the other hand the p38α MAPK is responsible for different inflammatory responses and thus has become a well-established target for some chronic inflammatory diseases as rheumatoid arthritis [3], inflammatory bowel disease [4] and psoriasis [5]. Recently, several clinical trials investigating the benefit of p38α MAPK inhibitors for the treatment of chronic obstructive pulmonary disease were terminated [6, 7]. In addition, some studies have also highlighted p38α MAPK as a key protein in the pathogenesis of neurodegenerative diseases including AD, PD and multiple sclerosis [8-10]. As a consequence, great efforts have been focused in finding inhibitors for both JNK3 and p38α MAPK [11-13], which led to the achievement of molecules endowed with a good potency, although often lacking a satisfactory selectivity.

JNK3 and p38α MAPK are both activated in response to environmental stress stimuli as well as pro-inflammatory cytokines and take part in different signaling pathways [14-17]. The activation is carried out by upstream MAPK kinases MKK4/MKK7 and MKK3/MKK6 for JNK3 and p38α MAPK, respectively, via a concomitant phosphorylation of a threonine and a tyrosine residues situated at the activation loop [15, 18]. Amongst others, the most evident conformational modification following is the shift of a tripeptide Glu-Phe-Gly situated at the beginning of the activation loop, known as DFG motif, from an "out" conformation on the inactive enzyme to an "in" conformation [19]. Such modification has been well characterized and widely described for p38α MAPK [20, 21] and recently, the possible adoption of the DFG-out conformation has been reported for JNK3 as well [22]. The majority of the p38α MAPK inhibitors and almost all of the reported JNK3 inhibitors discovered so far are classified as type I inhibitors, binding at the adenosine triphosphate (ATP) binding site of the enzyme in its active conformation and thus being ATP competitive [23]. However, most of type I inhibitors are also able to bind to the inactive form of the enzyme, probably due to the fact that the position of the DFG motif doesn't affect the binding mode of these compounds [21, 24]. On the other side, type II inhibitors bind the ATP cleft of the inactive enzyme, exploiting a hydrophobic pocket known as the deep pocket, which is only present in the DFG-

out conformation [25]. Since the inactive form of the kinase is not able to bind ATP, this modality of binding avoids the competition with high intracellular ATP concentrations. Furthermore, as the amino acid composition of the deep pocket is low conserved within the catalytic site of related kinases, type II binding allows to achieve an improved selectivity profile. Despite the high desirability of MAPK type II inhibitors, only a few of these inhibitors have been characterized for p38α MAPK [26], whereas to date, no type II inhibitors have been reported for JNK3.

The activity of type I inhibitors on JNK3 and p38α MAPK is generally evaluated through biological assays quantifying the amount of MAPK substrate phosphorylated from the active enzymes in presence and absence of the inhibitor [27, 28]. These activity assays provide an exhaustive indication about the inhibitory activity of compounds but are generally expensive, time consuming, and not amenable for high throughput screening (HTS) due to multiple separation and washing steps. The evaluation of type II inhibitors is instead far more challenging, albeit some screening assays for inactive p38α MAPK have been reported in the last years [29, 30]. An additional strategy in the identification of new kinase inhibitors is the detection of the binding affinity of novel compounds for the enzymes, which is a substantial prerequisite for any inhibitory activity. With this scope, herein we report the development and optimization of fluorescence polarization (FP)-based competition binding assays, which employ a novel fluorescein-labelled probe binding to both the active and inactive conformations of JNK3 and p38α MAPK. The FP is a technique increasingly used within the last years in the field of drug discovery, due to its several advantages as versatility, speed, easy handling and cost efficiency [31, 32]. It is even useful for detecting weak binding events only limited by compound solubility [33]. The basic principle of this methodology is that after excitation by plane polarized light the fluorophore's emission is polarized as well due to photoselection. However, the capability of the fluorophore to retain such polarization depends on its molecular size. Small molecules, as the fluorophore alone, are prone to fast tumbling due to Brownian motions. Therefore the light emitted loses easily the polarization achieved and produces low FP signal. On the other hand, the FP signal dramatically

increases when the fluorophore binds to a protein, due to a slower tumbling of the high molecular weight complex. As a result, the displacement of a fluorescent probe from the enzyme by a tested compound can be followed by measuring the FP signal directly after the addition (mix and measure) without separation and washing steps. This feature, together with a significantly improved safety, makes the FP-based binding assay superior in comparison to traditional binding assays based on radioligands. [34, 35].

The herein presented assay, using slightly different conditions, has been recently employed from our group on the wildtype form as well as on gatekeeper mutations of JNK3 [36] and represents the first example of an FP-based binding assay on JNK3. On the other side Munoz *et al.* reported in 2010 an FP competition assay for the inactive form of the p38α MAPK [37]. The probe employed in this assay (compound **2**, Fig. 1) is based on the prototypical p38α MAPK inhibitor SB203580, which was modified on its side chain and labelled with the 4'-isomer of fluorescein isothiocyanate (FITC). However, the FP-assay reported by Munoz *et al.* does not show correlation with the p38α MAPK activity assay (R^2 = -0.4005) [37].

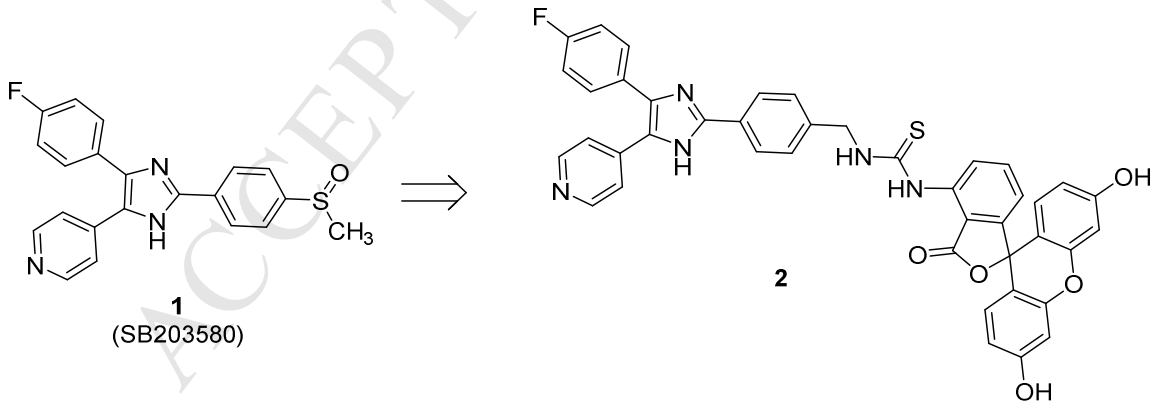

Fig. 1. Reported probe for p38α MAPK FP assay based on the p38α MAPK prototype inhibitor SB203580.

Herein, we describe the development of two novel and wider applicable probes (compounds **5** and **6**, Fig. 2) due to their derivation from dual JNK3/p38α MAPK inhibitors (compounds **3** and **4**, Fig. 2). Two analogous binding assays employing the inactive form of both, JNK3 and p38α MAPK, using the most promising probe **5** were optimized. The use of the inactive form of both kinases enhances the application spectrum of these assays since it enables the evaluation of binding affinity for type I as well as type II inhibitors. The results obtained from the binding assays were correlated with the ones obtained from enzyme-linked immunosorbent assay (ELISA) activity assays and the viability of the optimized protocols in a HTS format was investigated.

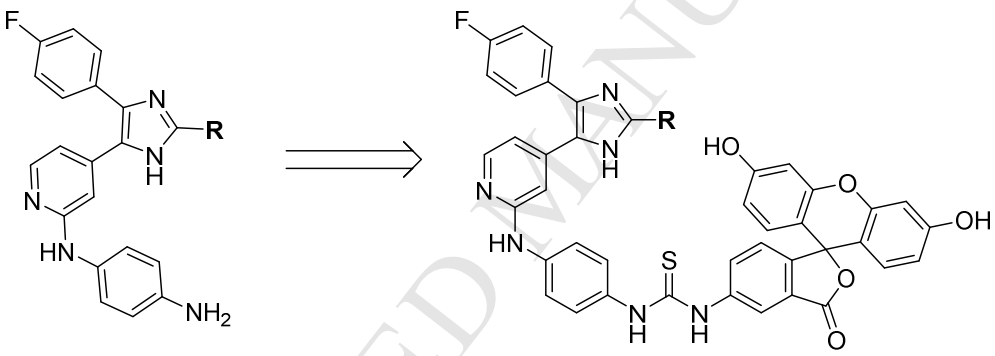

Fig. 2. Novel probes for JNK3 and p38α MAPK FP assay based on potent dual JNK3/p38α MAPK inhibitors **3** and **4**.

2. Materials and methods

2.1 Computational docking analysis

2.1.1 Molecule and Binding Pocket Preparation for Docking

To prepare molecules for docking we used the Molecular Operating Environment (MOE) suite's "molecule wash" function to deprotonate strong acids and protonate strong bases

(MOE 2013.08; Chemical Computing Group Inc., 1010 Sherbooke St. West, Suite #910, Montreal, QC, Canada, H3A 2R7, 2015). Energy minimization of all molecules was then performed by using the MMFF94x force field at a gradient of 0.0001 root-mean-square deviation (rmsd). Existing chirality was preserved and partial charges were calculated according to the parameters of the force field.

All crystal structures (3FI3 and 1OUK) [38, 39] were downloaded from the Protein Data Bank (PDB) [40]. Subsequently, protonation of the protein–ligand complex was performed with the MOE 'Protonate 3D' function at standard settings (T = 300 K, pH = 7.0, ionic strength I = 0.1 mol/L).

2.1.2 Docking Experiments

All docking experiments were performed using the docking program GOLD (GOLD, version 5.2.2; The Cambridge Crystallographic Data Centre, Cambridge, UK, 2013) in combination with the scoring functions ChemPLP [41] and GoldScore [42] for 3FI3 and the combination of GoldScore and ChemScore [43] for 1OUK. The search efficiency for the genetic algorithm was increased from standard 100% to 200% at automatic mode. Binding site residues were defined by specifying crystal structure ligand coordinates, the active site radius setting remained at a default value of 6 Å with the „detect cavity" option enabled. For each target, we employed a test docking of the ligand from the crystal structure into its binding pocket. If pose retrieval was unsatisfying, we optimized docking parameters and continued with the best settings in respect of pose retrieval.

2.2 Probes Synthesis

2.2.1 General

All reagents and solvents were of commercial quality and utilized without further purification. Thin layer chromatography (TLC) reaction controls were performed for all reactions using fluorescent silica gel 60 F_{254} plates (Merck) and visualized under natural light and UV illumination at 254 and 365 nm. The purity of all synthesized probes and tested compounds

are >95% as determined via reverse phase high performance liquid chromatography (HPLC) on a Hewlett Packard HP 1090 Series II LC equipped with a UV diode array detector (DAD, detection at 230 nm and 254 nm). The chromatographic separation was performed on a Phenomenex Luna 5u C8 column (150 mm x 4.6 mm, 5 µm) at 35 °C oven temperature. The injection volume was 5 µL and the flow 1.5 mL / min using the following gradient: 0.01 M KH_2PO_4, pH 2.3 (solvent A), methanol (solvent B), 40% B to 85% B in 8 min; 85% B for 5 min; 85% to 40% B in 1 min; 40% B for 2 min; stop time 16 min. Column chromatography was performed on Davisil LC60A 20 - 45 µm silica from Grace Davison and Geduran Si60 63-200 µm silica from Merck for the pre-column using an Interchim PuriFlash 430 automated flash chromatography system. Nuclear magnetic resonance (NMR) spectra were measured on a Bruker Avance NMR spectrometer at 250 MHz in the Organic Chemistry Institute, Eberhard Karls Universität Tübingen or on a Bruker Avance 400 NMR spectrometer in the Institute of Pharmaceutical Sciences, Eberhard Karls Universität Tübingen. Chemical shifts are reported in parts per million (ppm) relative to tetramethylsilane. All spectra were calibrated against the (residual proton) peak of the deuterated solvent used. Mass spectra were performed on an Advion Expression S electrospray ionization mass spectrometer (ESI-MS) with TLC interface in the Institute of Pharmaceutical Sciences, Eberhard Karls Universität Tübingen.

2.2.2 Experimental procedures

N1-(4-(4-(4-Fluorophenyl)-2-(methylthio)-1*H*-imidazol-5-yl)pyridin-2-yl)benzene-1,4-diamine (3)

In a pressure tube compound **8** (500 mg, 1.65 mmol) and *p*-phenylendiamine (267 mg, 2.47 mmol) were suspended in *n*-butanol (10 mL) and then 1.25 M HCl in ethanol (1.32 mL, 1.65 mmol) was added. After sealing the tube, the mixture was stirred at 180 °C for 16 h. The solvent was evaporated at reduced pressure and the residue was purified by flash column chromatography (dichloromethane – ethanol 19:1 to 93:07) giving 568 mg of product (88%). ^{1}H NMR (400 MHz, DMSO-d_6) δ (ppm) 2.61 (s, 3H,), 4.74 (br s, 2H), 6.49 (d, J = 7.1 Hz, 2H),

6.53 - 6.96 (m, 2H), 7.11 (d, *J* = 7.1 Hz, 2H), 7.16 - 7.37 (m, 2H), 7.50 (br s, 2H), 7.80 - 8.11 (m, 1H), 8.24 - 8.54 (m, 1H), 12.65 (br s, 1H); HPLC: t = 3.36 min, 98%; ESI-MS: $[M+H]^+$ calculated 392.13, found 392.2.

1-(3',6'-Dihydroxy-3-oxo-3*H*-spiro[isobenzofuran-1,9'-xanthen]-5-yl)-3-(4-((4-(4-(4-fluorophenyl)-2-(methylthio)-1*H*-imidazol-5-yl)pyridin-2-yl)amino)phenyl)thiourea (5)

A suspension of **3** (200 mg, 0.51 mmol) and FITC isomer 5' (298 mg, 0.76 mmol) in acetone (60 mL) was stirred at room temperature (r.t.) for 24 h covered from light. The solvent was evaporated at reduced pressure and the residue was purified by flash column chromatography (dichloromethane – ethanol 19:1 to 4:1) giving 207 mg of the desired compound (52%). ^{1}H-NMR (250 MHz, DMSO-d_6) δ (ppm) 2.62 (s, 3H), 6.55 - 6.85 (m, 7H), 7.05 - 7.35 (m, 6H), 7.45 - 7.65 (m, 4H), 7.83 (d, *J* = 8.2 Hz, 1H), 7.95 - 8.15 (m, 1H), 8.20 (br s, 1H,), 9.10 (br s, 1H), 9.95 - 10.25 (m, 4H), 12.70 (br s, 1H); HPLC: t = 6.19 min, 95%; ESI-MS: $[M-H]^-$ calculated 779.85, found 779.5.

2-Fluoro-4-(4-(4-fluorophenyl)-1*H*-imidazol-5-yl)pyridine (11)

Compound **10** (2.00 g, 8.09 mmol) was dissolved in DMF (5 mL) and then formaldehyde (243 mg, 8.09 mmol), ammonium acetate (6.23 g, 80.9 mmol) and glacial acetic acid (47 mg, 0.81 mmol) were added and the mixture was stirred at 70 ℃ for 1 h. The reaction mixture was poured into water and the precipitate formed was filtered, washed with water and dried. The solid was then purified by column chromatography (dichloromethane – ethanol 97:3 to 4:1) yielding 200 mg (10%) of **11**.

Spectroscopic data were in agreement with those in the literature [44]**.**

N1-(4-(4-(4-Fluorophenyl)-1*H*-imidazol-5-yl)pyridin-2-yl)benzene-1,4-diamine (4)

In a pressure tube, compound **11** (150 mg, 0.58 mmol) and *p*-phenylendiamine (315 mg, 2.91 mmol) were suspended in *n*-butanol (3 mL) and then 1.25 M HCl in ethanol (0.46 mL, 0.58 mmol) was added. After sealing the tube, the mixture was stirred at 180 ℃ for 16 h. The

solvent was evaporated *in vacuo* and the residue was purified twice by column chromatography (dichloromethane – ethanol 19:1 to 4:1) giving 124 mg of product (60%).

^{1}H-NMR (250 MHz, DMSO-d_6) δ (ppm) 4.75 (br s, 2H), 6.46 (d, J = 8.6 Hz, 2H), 6.60 (dd, J_1 = 5.3 Hz, J_2 = 1.2 Hz, 1H), 6.77 (br s, 1H), 7.06 (d, J = 8.6 Hz, 2H), 7.20 - 7.30 (m, 2H), 7.45 - 7.55 (m, 2H), 7.80 (s, 1H), 7.95 (br s, 1H), 8.35 (br s, 1H), 12.60 (br s, 1H); ESI-MS: $[M+H]^+$ calculated 346.38, found 346.3; $[M-H]^-$ calculated 344.38, found 344.3.

1-(3',6'-Dihydroxy-3-oxo-3*H*-spiro[isobenzofuran-1,9'-xanthen]-5-yl)-3-(4-((4-(4-(4-fluorophenyl)-1*H*-imidazol-5-yl)pyridin-2-yl)amino)phenyl)thiourea (6)

A solution of compound **4** (70 mg, 0.20 mmol) and FITC isomer 5' (118 mg, 0.30 mmol) in acetone (20 mL) was stirred at r.t. for 24 h. The reaction mixture was concentrated to dryness and the residue was purified by column chromatography (dichloromethane – ethanol 9:1 to 1:1) to yield 60 mg (40%) of product **6**. ^{1}H-NMR (250 MHz, DMSO-d_6) δ (ppm) 6.50 - 6.67 (m, 6H), 6.73 (d, J = 5.5 Hz, 1H), 7.05 - 7.35 (m, 7H), 7.45 - 7.60 (m, 4H), 7.80 - 7.87 (m, 2H), 8.05 (br, 1H), 8.26 (br, 1H), 9.05 (br, 1H), 10.00 - 10.60 (m, 4H), 12.52 (br, 1H); HPLC: t = 3.77 min, 96%; ESI-MS: $[M-H]^-$ calculated 733.76, found 733.4.

2.3 Expression and purification of inactive JNK3 and inactive p38α MAPK

Inactive JNK3 and p38α MAPK were expressed and purified following the procedure previously reported by Lange *et al*. [36].

2.4 Activity assay

Probes **5** and **6** as well as compounds **1**, **3** and **12**-**22** were tested for their inhibitory activity for JNK3 and/or p38α MAPK in previously reported ELISA activity assays [27, 28].

2.5 FP assay

2.5.1 General

All FP measurements were performed in black, non-binding 96-well plates (Greiner Bio-One) and conducted through a CLARIOstar microplate reader (BMG Labtech GmbH) using

excitation and emission filters of 480 nm and of 530 nm, respectively. For JNK3 measurements buffer A (25mM HEPES pH 7.0, 100 mM NaCl, 2 mM $MgCl_2$, 10 mM β-mercaptoethanol (BME) and 0.05 mg/ml bovine serum albumin (BSA)) was used, whereas buffer B (25 mM Tris pH 7.1, 100 mM NaCl, 10 mM $MgCl_2$, 5 mM DTT, 5% glycerol, 0.05 mg/ml BSA) was employed in the assay performed on p38α MAPK. The concentration of DMSO used in every assay was 5% (v/v) and the final volume in every well was 200 µL. Incubation was carried out for the respective time at r.t. on an Eppendorf MixMate at 400 revolutions per minute (rpm) including 2 min inside the plate reader in order to equilibrate at the measurement temperature (25 ℃ for JNK3 and 28 ℃ for p38α MAPK) which only deviated marginally from the incubation temperature. Before every measurement, the focal height of the excitation beam was tuned in order to achieve the optimal fluorescence intensity and the gain value for both detectors was adjusted. All experiments were performed three times in quadruplicate. Absolute polarization values were normalized to the average values of first well and last well replicates and reported as percentage. Data were fitted to a four-parameter logistic curve with variable slope using the software GraphPad Prism 4 (GraphPad Prism 4, GraphPad Software Inc., San Diego, CA, USA). K_i values for the competition assays were calculated from the measured IC_{50} values using a modified Cheng-Prusoff equation from the group of Shaomeng Wang [45, 46].

2.5.2 Probes characterization and time stability

A final concentration of 10 nM of probes **5** and **6** was titrated with 3-fold increasing concentrations of JNK3 and p38α MAPK, ranging from 0 to 600 nM. Concentrations used for both kinases were 0 nM, 0.01 nM, 0.03 nM, 0.09 nM, 0.27 nM, 0.82 nM, 2.47 nM, 7.40 nM, 22.22 nM, 66.66 nM, 200 nM and 600 nM. Prior to the reading, plates were incubated for a total time of 15, 30 and 60 min.

2.5.3 Assay conditions optimization

A final concentration of 5 nM of probe **5** was titrated with 3-fold increasing concentrations of JNK3 and p38α MAPK, ranging from 0 to 300 nM. Concentrations used for both kinases

were 0 nM, 0.005 nM, 0.015 nM, 0.045 nM, 0.13 nM, 0.41 nM, 1.23 nM, 3.70 nM, 11.11 nM, 33.33 nM, 100 nM and 300 nM. The FP was measured after a total time of incubation of 30 min.

2.5.4 Autofluorescence assay

Prior to the measurement, compounds **1**, **3** and **12**-**23** were tested for their fluorescence intensity at the excitation and emission wavelengths of 480 nm and 530 nm, respectively, using a concentration of 1 μM of the test compound in buffer A. Buffer A containing 5% DMSO (v/v) served as a negative control whereas two different concentrations of probe **5** (5 nM and 1 μM) in the same buffer were used as positive controls.

2.5.5 Competition binding assay

A final concentration of 10 nM of the respective protein kinase and 5 nM of probe **5** were measured after addition of increasing concentrations of compounds **1**, **3**, **12**-**16**, **18** and **20**-**23** (11 different concentrations including a well without inhibitor). For each measurement, a well containing a 5 nM concentration of probe **5** in buffer was included as a negative control. The range of compounds concentrations was selected in order to achieve a full sigmoidal curve. The FP signal was measured after an incubation time of 30 min. Linear regression on plotted logarithmic results of the FP assay and the ELISA assay was calculated using GraphPad Prism 4.

2.5.6 HTS assay validation

The suitability for HTS of the competition binding assays on JNK3 and p38α MAPK was evaluated following NCBI guidelines manual [47]. The interleaved-signal format described was employed. For the assays, a 10 nM concentration of the enzyme in the respective assay buffer and a 5 nM concentration of probe **5** were employed in every well. 5% (v/v) of DMSO was constantly used in all the assay plates. As a negative control for both enzymes probe **5** alone at the aforementioned concentration was chosen. In the JNK3 experiments, compound **3** at a concentration of 1 μM was employed as a positive control whereas the same

compound at 20 nM concentration was used as middle control. Regarding the p38α MAPK, the same compound (**3**) was employed at concentrations of 2 μM and 50 nM for the positive and middle control, respectively. The experiment was performed three times in three different days: controls were plated in a black, non-binding 96-well plate following the scheme reported in literature [47] and the FP signal was read after 30 min incubation at r.t. The measurement was carried out at 25 ℃ and the focus height and the gain values were adjusted before every measurement. Percent coefficient of variation (%CV) for the negative, positive and middle controls were calculated for each plate. Each single well signal of middle control was normalized to the mean of negative and positive controls of the same plate in order to achieve a percentage of activity. After that, mean and standard deviation (SD) for the middle control were calculated on the normalized values. Finally, the Z-factor of every plate was calculated. The single well signals of each day were plotted separately in graphs "by row, then column" and "by column, then row", using the software Prism 4, in order to detect drift or edge effects.

2.6 Isothermal titration calorimetry (ITC)

A reverse ITC was performed due to the lack of solubility of compounds to be tested. 10 mM solutions of probe **5** and **6** in DMSO were diluted 1:100 with pure DMSO and eventually further diluted 1:20 with buffer C (50 mM Hepes pH 7.0, 100 mM NaCl, 2 mM $MgCl_2$ and 2 mM tris(2-carboxyethyl)phosphine (TCEP)) for JNK3 and with buffer D (25 mM Tris pH 7.1, 100 mM NaCl, 10 mM $MgCl_2$ and 1 mM BME) for p38α MAPK in order to achieve a 4 μM concentration of compound with a 5% (v/v) final DMSO concentration. The aforementioned solutions were loaded into the sample cell of a MicroCal ITC200 (former GE Healthcare, now Malvern). A freshly concentrated solution of JNK3 or p38α MAPK in buffer C or D, respectively, containing a 5% (v/v) DMSO concentration, was loaded in the titration syringe. Measurements were performed at 25 ℃. Protein solut ion was titrated into the sample cell in 20 injection steps of 2 μL each, at a rate of 0.5 μL/s with an interval of 120 s between the steps. Stirring was applied at 1000 rpm. Before the first step, 0.5 μL of protein solution was

injected into the sample cell, in order to correct for protein diffusion from the syringe during experimental set up and equilibration. The data point of this pre-step was neglected during data analysis. Data analysis was performed using MicroCal Origin software (Origin v. 7.0552, OriginLab Corporation, Northampton MA, USA).

3. Results

3.1 Design, synthesis and characterization of probes 5 and 6

As a starting point for the design of the two probes, the two pyridinylimidazoles **3** and **4** were selected as precursor molecules (Fig. 2). Both compounds were identified in a current ongoing research program as potent dual inhibitors of JNK3 and p38α MAPK (Table 1). The *p*-phenylendiamino group present in both compounds was chosen for the linking of the fluorescein tag. Computational docking studies of **3** with both kinases (Fig. S1, supplementary material) as well as comparison of the binding mode with similar pyridinylimidazole and pyrimidinylimidazole-based kinase inhibitors [38, 48, 49] revealed that this portion of the molecule occupies the hydrophobic region II of the enzyme. This is an area of the ATP binding pocket that is solvent exposed and thus supposed to be able to tolerate the bulkiness of the fluorescein moiety. In contrast to the previously reported probe **2** by Munoz *et al*. (Fig. 1) [37], we chose the more easily available 5'-isomer of FITC as a starting material to insert the fluorophore. The design hypothesis of our probes was supported by computational docking studies of compound **5** with both enzymes showing the bulky fluorescein group ranging outside the enzyme and therefore presumably not hampering the binding (Fig. S2, supplementary material).

The first probe, compound **5**, was synthesized as depicted in Scheme 1 starting from known 2-chloro-4-(4-(4-fluorophenyl)-2-(methylthio)-1*H*-imidazol-5-yl)pyridine (**8**). Pyridinylimidazole **8**, which is synthetically accessible from the commercially available 2-chloro-4-methylpyridine (**7**) in four synthetic steps [50], was subsequently reacted in a nucleophilic aromatic substitution reaction with *p*-phenylendiamine to obtain compound **3**. The precursor **3** was

labeled with the fluorophore through the formation of a thiourea group between the primary amino group and the 5'-isomer of FITC at r.t.

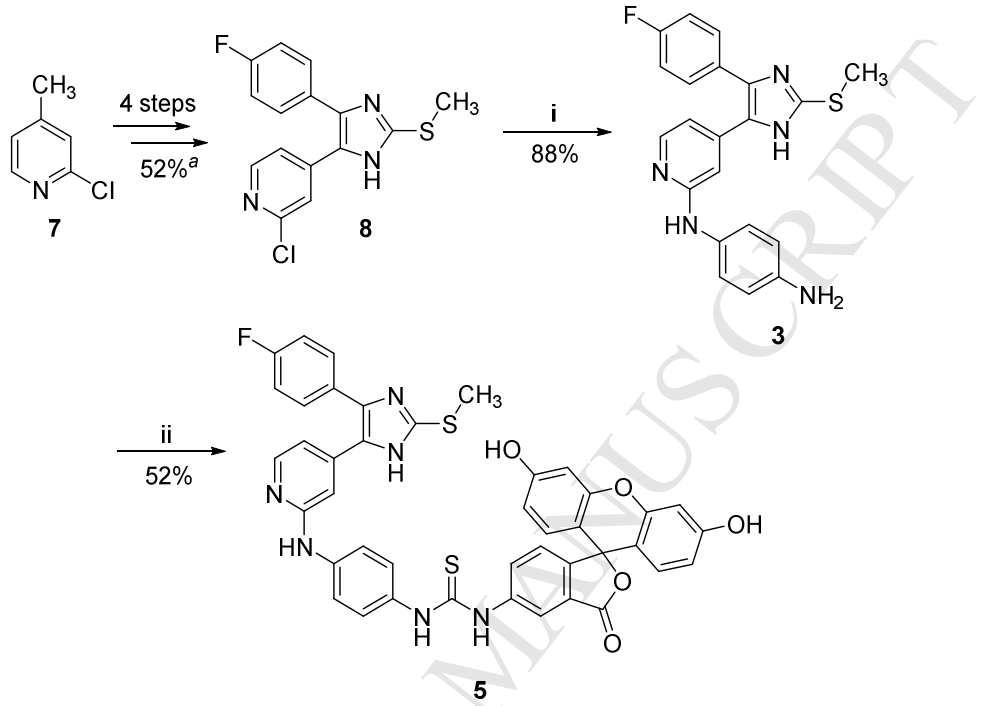

Scheme 1. Synthesis of the probe **5** starting from 2-chloro-4-methylpyridine (**7**). Reagents and conditions: (i) *p*-phenylendiamine, HCl in ethanol 1.25 M, *n*-butanol, 180 ℃, 16 h; (ii) FITC isomer 5', acetone, r.t., 24 h; [a]yield derived from Laufer *et al.* [50].

The second probe, compound **6** (PIT0105016 in our previously published work [36]) was prepared starting from already reported ethane-1,2-dione **10**, which was synthesized according to our reported protocol in two steps from 2-fluoro-4-methylpyridine (**9**) (Scheme 2) [51]. Cyclization under Radziszewski conditions [52] of dione **10** using ammonium acetate and formaldehyde provided pyridinylimidazole **11**. Finally, the substitution with *p*-phenylendiamine as well as the introduction of the fluorophore yielding probe **6** were performed using the same conditions as described for probe **5**.

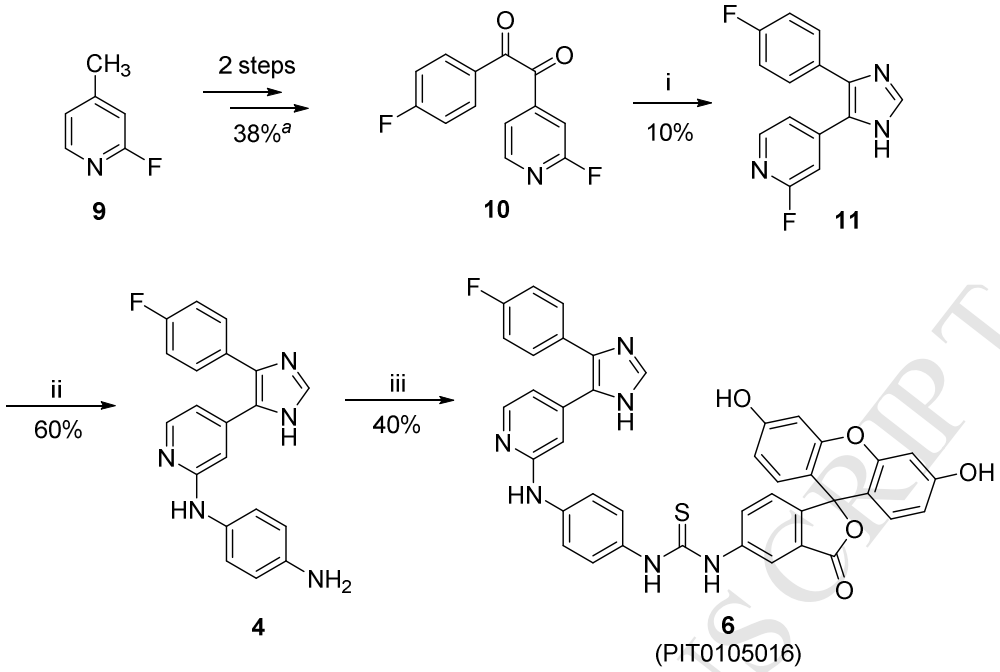

Scheme 2. Synthesis of probe **6** starting from 2-fluoro-4-methylpyridine (**9**). Reagents and conditions: (i) formaldehyde, NH_4OAc, acetic acid, dimethylformamide (DMF), 70 ℃, 1 h; (ii) *p*-phenylendiamine, HCl in EtOH 1.25 M, *n*-butanol, 180 ℃, 16 h; (iii) FITC isomer 5', acetone, r.t., 24 h; [a]yield derived from Koch *et al.* [51].

Probes **5** and **6** were also tested for their ability to inhibit JNK3 and p38α MAPK showing only a negligible decrease in potency in comparison with the unlabeled precursors **3** and **4** (Table 1). This demonstrates the low impact of the fluorescent moiety on the binding affinity, confirming our design hypothesis as well as the results of the docking studies.

The insertion of a further spacer between the fluorescein moiety and the *p*-phenylendiamino group was therefore considered unnecessary and potentially detrimental, since a higher flexibility of the fluorescein-labelled probe could cause a decrease in the width of the signal window [53].

Table 1. Biological activity of precursors **3** and **4** and probes **5** and **6** tested in ELISA activity assays.

Cpd.	IC_{50} ± SEM[a] (nM)	
	JNK3	p38α MAPK
3	24 ± 1	17 ± 0
4	4.7 ± 0.4	7.5 ± 0.3
5	48 ± 2	26 ± 0
6	74 ± 1	29 ± 2

[a]n = 3.

3.2 K_d determination of probes

With the aim to estimate the binding of the two probes to the inactive form of the protein kinases, a fixed concentration of 10 nM of probes **5** and **6** was titrated with increasing concentrations of JNK3 and p38α MAPK (0 – 600 nM). The FP signal was read after incubation at r.t. for 15, 30 and 60 min, thus allowing also to evaluate the time dependence of the experiment in terms of equilibrium onset and signal stability. Non-linear fit of the data obtained in the titration experiment of the two probes (Fig. 3) resulted in very close K_d values in the low single-digit nanomolar range for both kinases (Table 2). Due to a very similar binding profile of the two compounds, the selection of probe **5** for the further optimization of the assays relied mainly on a higher overall yield of the synthetic route (23% in case of probe **5** versus 1% in case of probe **6**, compare Scheme 1 vs. Scheme 2). Regarding the time dependence of the assays, both probes showed in both enzymes only a small variation in K_d value (≤1.3 nM) between 15 and 60 min. This suggests a rapid onset of the binding equilibrium of the probes that is already reached after 15 min. Nevertheless, since an incubation time of 30 min was considered more suitable in binding competition assays of inhibitors with unknown binding kinetic, the K_d values of the two probes after 30 min of incubation was selected as the K_d value to be considered in the competition assays.

Table 2. Binding affinities of probes **5** and **6** for JNK3 and p38α MAPK at different times of incubation tested in the FP assays.

Probe	K_d ± SEM[a] (nM)					
	JNK3			p38α MAPK		
	15 min	30 min	60 min	15 min	30 min	60 min
5	2.7 ± 0.2	3.0 ± 0.2	4.0 ± 0.3	5.4 ± 1.0	5.7 ± 1.1	6 .2 ± 1.2
6	2.3 ± 0.1	2.6 ± 0.1	3.2 ± 0.1	6.2 ± 0.1	6.5 ± 0.2	7 .2 ± 0.3

[a]n = 3; concentration of probe used was 10nM; total volume of DMSO was 5% (v/v).

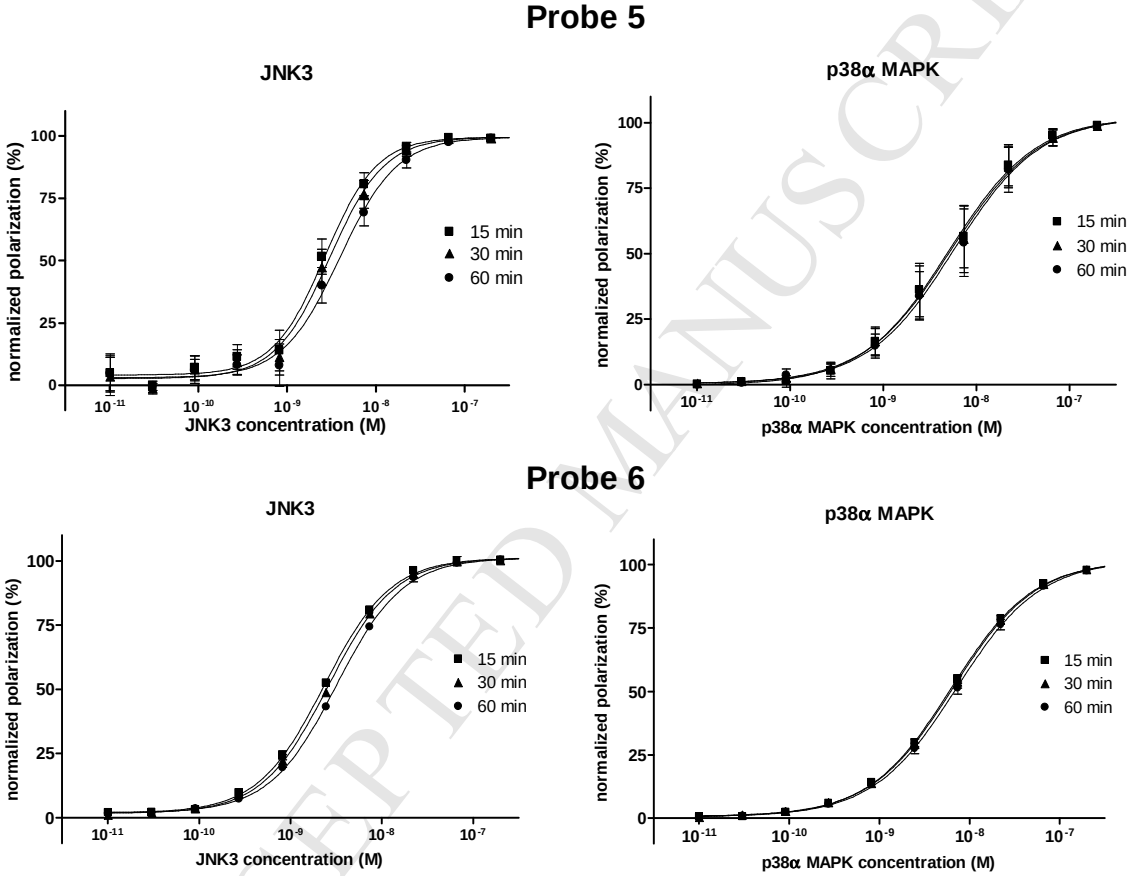

Figure 3. Titration of probes **5** and **6** with inactive JNK3 and inactive p38α MAPK. Probe concentration was 10 nM in 5% (v/v) DMSO. Data points represent mean values ± SD.

The K_d values of probes **5** and **6** were further determined using ITC as an additional technique. The K_d values (Table 3 and Fig. S3, supplementary material) obtained by ITC experiments for both probes are slightly higher compared to those obtained by direct titration in the corresponding FP assays, probably due to different intrinsic characteristics of the two

techniques and of the experimental protocols. Nevertheless, the high affinity of the probes for the two enzymes was again confirmed.

Table 3. Binding affinities of probes **5** and **6** for JNK3 and p38α MAPK determined by ITC.

Probe	K_d ± SEM[a] (nM)	
	JNK3	p38α MAPK
5	25 ± 5	35 ± 5
6	20 ± 1	33 ± 3

[a]n = 3; results were obtained through reverse ITC. Protein concentration in the titration syringe was 55 μM and compound concentration in the sample cell was 4 μM.

3.3 Assay conditions optimization

After determination of K_d values for probe **5** (Table 2), a concentration of 5 nM was selected as a final concentration to be used in the competition assays for both enzymes. This is in accordance with FP assay development guidelines [54], suggesting a probe concentration as low as possible, preferably not significantly higher than twice the probe K_d value. Using this probe concentration, a second titration with increasing concentrations of the two enzymes was performed in order to select the optimal protein concentration (Fig. S4, supplementary material). In line with practical considerations [54], such concentration should yield an increase in the polarization signal included between 50 and 80% of the overall signal window, thus giving a still significant width of signal and at the same time being far from stoichiometric conditions, in order to provide the assay with a better sensitivity. A concentration of 10 nM of both enzymes yielding signal windows of ≈140 mP and ≈165 mP for JNK3 and p38α MAPK, respectively, was therefore selected as the standard concentration employed in the competition assays.

3.4 Assay validation and correlation

With the purpose of validating the optimized assays, as well as assessing their viability in predicting the potency of type I inhibitors in reference activity assays, a series of 13 compounds (Fig. 4) was selected to be evaluated for JNK3 and/or p38α MAPK for their capability to displace the fluorescein-labelled probe **5**. This series consists of different pyridinylimidazoles from our compound library [55, 56] including the non-labelled precursor of probe **5** (compound **3**), as well as the two p38α MAPK reference compounds SB203580 (**1**) and ML3403 (**12**). In order to demonstrate the full capacity of the probe, examples of non pyridinylimidazole-type kinase inhibitors were also selected to be investigated. The early JNK3 inhibitor SP600125 (**17**) [57], aminopyrimidine **18** [36] and clinical candidate AS601245 (**19**) [58] were chosen for the assay on JNK3, whereas high quality kinase probe Skepinone-L (**21**) [59] as well as clinical candidate SB681323 (**22**) [60] were tested on p38α MAPK. Finally, pyridinylquinoxaline **20** [51] was tested on both enzymes. All compounds were previously evaluated in ELISA activity assays (IC_{50} values are shown in Table 3) and were then chosen in order to achieve, within the series, a range of different activities for both enzymes.

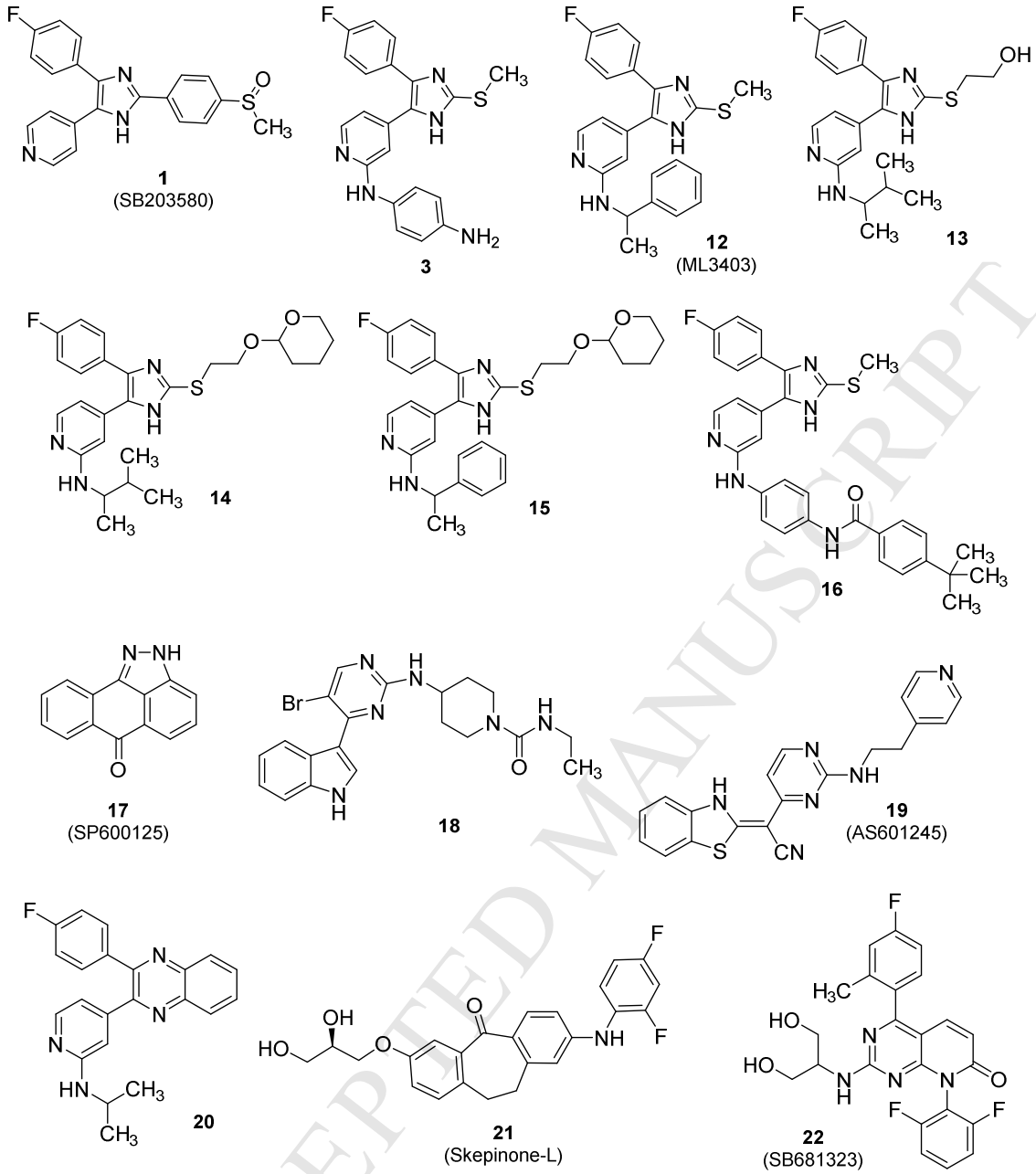

Fig. 4. Structures of tested compounds.

All selected compounds were primarily tested for autofluorescence at the absorption and emission wavelengths used for the fluorescein-labelled probe, in order to ensure that the measured FP signal could be exclusively attributable to the probe. One of the drawbacks of FP assay indeed, is its unsuitability for the evaluation of compounds showing autofluorescence at the same wavelengths employed for the fluorophore [53]. For this reason SP600125 (**17**) and AS601245 (**19**), which displayed a fluorescence comparable to the

positive control (5 nM probe), had to be excluded from the assay (data not shown). In order to achieve for every measurement a complete displacement of the labelled probe, compounds were tested at different ranges of concentrations depending on their ability to bind the two protein kinases. The IC_{50} values resulting from the competition binding assays were then converted into K_i values through a modified Cheng-Prusoff equation [45, 46] (Table 4).

Table 4. Comparison of activity of tested compounds on the ELISA assays and the FP assays.

	JNK3		p38α MAPK	
Cpd.	**activity assay IC_{50} ± SEM[a] [nM]**	**FP binding assay K_i ± SEM[a] [nM]**	**activity assay IC_{50} ± SEM[a] [nM]**	**FP binding assay K_i ± SEM[a] [nM]**
1	727 ± 28[b]	167 ± 10	50 ± 0.4[c]	56 ± 1
3	24 ± 1	3 ± 0.2	17 ± 0.4	14 ± 2
12	176 ± 2	40 ± 6	40 ± 5[d]	38 ± 1
13	181 ± 4	13 ± 1	11 ± 0.9[e]	4 ± 1
14	370 ± 13	49 ± 2	53 ± 4	39 ± 9
15	742 ± 12	142 ± 18	170 ± 10	141 ± 10
16	67 ± 2	5 ± 1	97 ± 8	61 ± 7
18	147 ± 5	29 ± 2	n.t.[f]	n.t.
20	3,950 ± 200[g]	1,041 ± 32	81 ± 5[g]	350 ± 10
21	n.t.	n.t.	5 ± 2[h]	4.2 ± 0.4
22	n.t.	n.t.	13 ± 0.1	7 ± 0.1

[a]n = 3. [b] data previously reported by Goettert *et al.* [27]; [c]data previously reported by Goettert *et al.* [28]; [d]data previously reported by Laufer *et al.* [61]; [e]data previously reported by Koch *et al.* [56]; [f]n.t., not tested; [g]data previously reported by Koch *et al.* [51] [h]data previously reported by Fischer *et al.* [62].

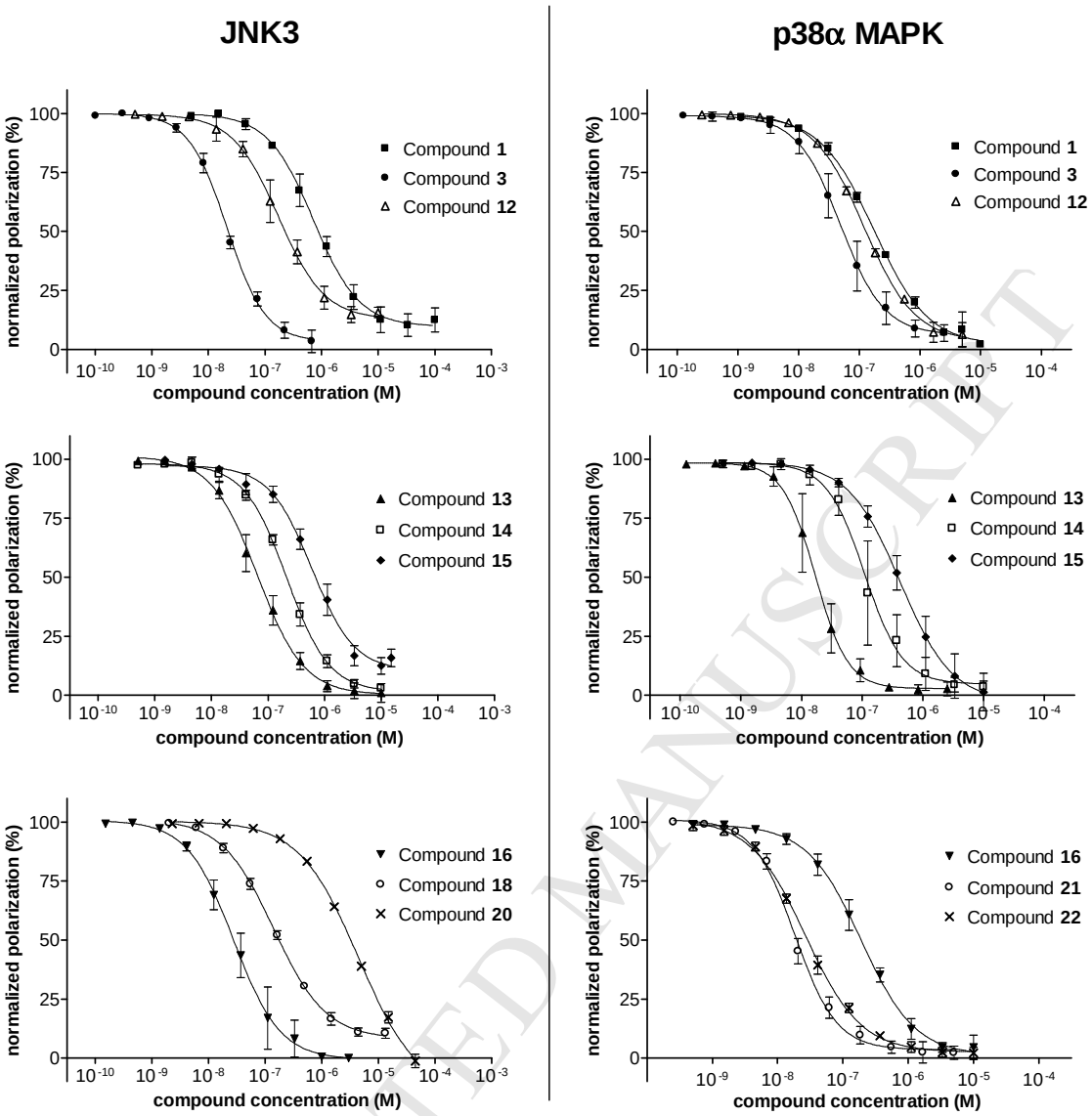

Fig. 5. Results of competition binding assays for the selected compounds. Probe **5** concentration was 5 nM and the concentration of enzyme was 10 nM. Data points represent mean values ± SD.

As displayed in Fig. 5, the assays are valid for both enzymes since the unlabeled precursor of probe **5** (compound **3**) as well as other tested inhibitors are able to displace the probe in a dose-dependent manner. Subsequently to the assay validation, the correlation between the herein presented FP-based binding competition assays and the ELISA activity assays was investigated. A correlation between these two assays could make the binding assays a useful tool for preliminary evaluation of new inhibitors of JNK3 and p38α MAPK in a fast and

relatively inexpensive manner with the aim to promote only better binders to a further characterization of the inhibition profile. Correlation was assessed through linear regression of the plotted logarithmic data for both assay methods (Fig. 6). With regard to JNK3, the enzyme activity assay and the FP-based competition binding assay proved to correlate remarkably (R^2 = 0.9555). In case of p38α MAPK, a good correlation was observed (R^2 = 0.8447), representing an advantage of our optimized p38α MAPK FP-assay in comparison to the existing one. These results display the suitability of both presented assays in the prediction of the inhibitory activity of novel compounds.

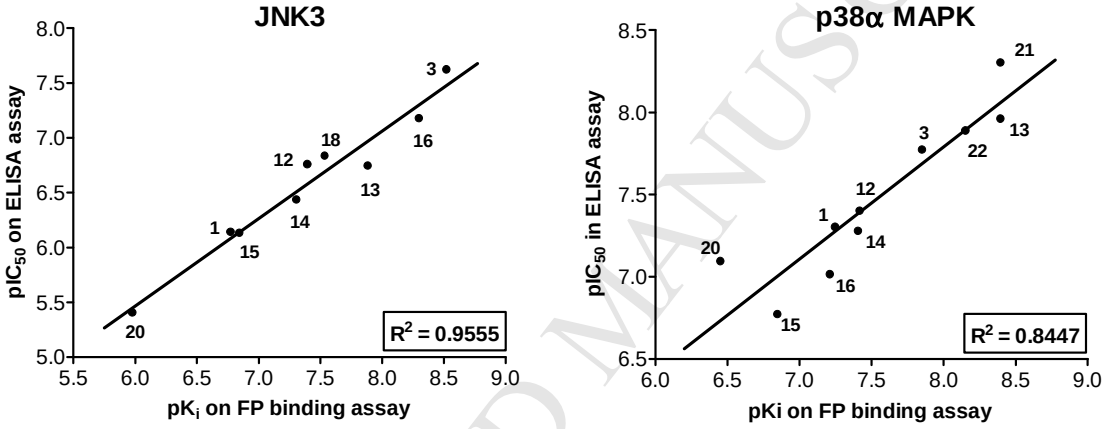

Fig. 6. Linear regression of plotted results for the ELISA activity assay and the FP competition binding assay.

As it is possible to observe from Table 4, the K_i values of the tested compounds are between low single-digit nanomolar range to low single-digit micromolar range. In order to estimate the limitation of binding affinity detection, a non-optimized inhibitor, namely 1-(4-fluorophenyl)-5-(pyridin-4-yl)imidazole (**23**), was tested as an example of a weak binder in both optimized FP-assays. Compound **23** displayed K_i values of 2,168 ± 29 nM and 24,030 ± 1,589 nM for JNK3 and p38α MAPK, respectively (Fig. 7). Binders of JNK3 and p38α MAPK with K_i values up to the low double-digit nanomolar range are detectable using the optimized FP-assay protocols presented.

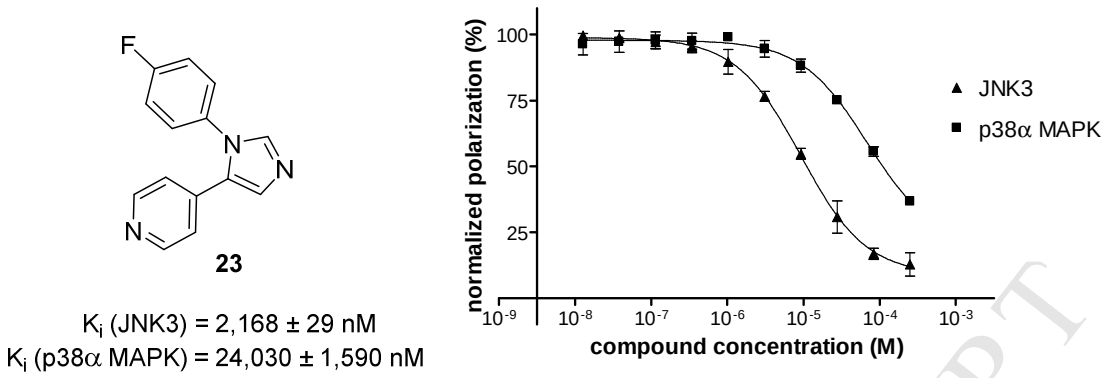

Fig. 7. Structure and binding affinity of 1-(4-fluorophenyl)-5-(pyridin-4-yl)imidazole (**23**).

3.5 HTS assay validation

The outcome of the experiments performed in section 3.4 prompted us to exploit the correlation between the binding and the activity assays on both enzymes for the rapid estimation of the (potential) inhibitory activity for large compounds sets. One of the advantages of FP assay is indeed the possibility to measure the signal directly after the addition of the components without washing or separation steps (mix and measure), which makes such assays suitable for the HTS format. In order to assess the viability of the FP assays developed for HTS, we followed the procedure reported in NCBI guidelines [47]. As a negative control probe **5** alone was selected. As a positive control the unlabeled probe (compound **3**), at a concentration known to displace the probe completely, was added to the same concentration of probe **5**. Finally, compound **3** was used as a middle control at a concentration close to its IC_{50} value. Results obtained (Table 5 and 6) were in agreement with the acceptance criteria described in the guidelines (%CV ≤ 20% for all controls, normalized SD for the middle control ≤ 20, low inter-plate variability of the normalized middle signal and Z-factor ≥ 0.4) and the plots of the single well values showed the absence of significant drift and edge effects (Fig. S5-S8, supplementary material) highlighting the suitability of these assays for HTS procedure.

Table 5. HTS assay validation results for JNK3.

#[a]	negative control		positive control		middle control			Z-factor
	FP value (mP) (mean ± SD)	%CV	FP value (mP) (mean ± SD)	%CV	FP value (mP) (mean ± SD)	%CV	Normalized activity (mean ± SD)	
1	300.3 ± 2.2	0.7%	161.7 ± 2.8	1.7%	220.8 ± 4.0	1.8%	42.6% ± 2.9%	0.89
2	300.5 ± 3.8	1.2%	151.3 ± 3.3	2.2%	210.7 ± 5.3	2.5%	39.8% ± 3.5%	0.86
3	298.0 ± 3.8	1.2%	143.1 ± 3.2	2.2%	195.1 ± 5.0	2.5%	33.5% ± 3.2%	0.86

[a]experiment number.

Table 6. HTS assay validation results for p38α MAPK.

#[a]	negative control		positive control		middle control			Z-factor
	FP value (mP) (mean ± SD)	%CV	FP value (mP) (mean ± SD)	%CV	FP value (mP) (mean ± SD)	%CV	Normalized activity (mean ± SD)	
1	296.1 ± 2.7	0.9%	122.4 ± 4.3	3.5%	256.9 ± 3.4	1.3%	77.4% ± 2.0%	0.88
2	304.9 ± 4.1	1.3%	134.9 ± 3.5	2.6%	226.9 ± 2.9	1.3%	54.1% ± 1.7%	0.86
3	291.9 ± 6.9	2.3%	124.9 ± 4.6	3.6%	214.6 ± 4.7	2.2%	53.7% ± 2.8%	0.79

[a]experiment number.

4. Discussion

The research for novel inhibitors of the two protein kinases JNK3 and p38α MAPK is still ongoing and aimed to the discovery of molecules displaying a high efficacy together with a satisfactory selectivity profile. A key approach might be represented by the identification of molecules, which bind preferentially the inactive conformation of these enzymes (type II inhibitors) taking advantage of binding pockets that are less conserved within the family of closely related kinases. With this scope, we developed two FP-based competition binding assays employing the inactive form of the two kinases able to measure the binding affinity of both type I and type II inhibitors. Classical activity assays using the active kinase exclude type II inhibitors predominantly binding to the inactive enzyme. Extending a previously reported assay for p38α MAPK, the herein presented assay broadens the range of

applicability including JNK3 due to the use of a dual JNK3/p38α MAPK inhibitor as a precursor of the probe employed. In addition, the comparison of the FP-assays presented with well-known ELISA activity assays allowed to observe a correlation between the two assays performed on both protein kinases. These results point out the potential of the assays presented as rapid and relatively inexpensive (low concentrations of kinase needed, no costly kinase substrates and antibodies required) alternatives to activity assays, which can be used to predict the inhibitory activity of new compounds in an early stage. Finally, the suitability of these assays to the HTS format allows the screening of wide libraries of compounds and therefore represents an improvement in the research of new JNK3 and p38α MAPK inhibitors.

5. Conclusion

The synthesis of two novel fluorescein-based pyridinylimidazoles and their evaluation for their ability to act as probes for the determination of binding affinity of kinase inhibitors to JNK3 and p38α MAPK is presented. Fast and inexpensive FP-assays for both enzymes using probe **5** (JNK3: K_d = 3.0 nM; p38α MAPK: K_d = 5.7 nM) were developed and validated with known inhibitors of JNK3 and p38α MAPK. The comparison of the results obtained from the FP-assays with the results of an ELISA-based activity assays revealed a good to excellent correlation, which makes the p38α MAPK FP-assay superior than the reported one. Moreover, both FP-assays are easily adaptable to the HTS procedure and therefore suitable as inexpensive pre-screening protocols for JNK3 and p38α MAPK inhibitors.

Acknowledgement

The authors thank Katharina Bauer and Daniela Müller who carried out the testing of the compounds in the activity ELISA assays. We are also grateful to Prof. Dr. Stefan Laufer for providing samples of SP600125, compound **18**, AS601245, Skepinone-L and SB681323. We thank Tamer Kocakaya and Philip Krause for synthesizing compounds **16** and **23**, respectively. Miriam Gisevius, Regina Jedig and Mark Kudolo (all students at the Institute of

Pharmaceutical Sciences, Eberhard Karls Universität Tübingen) are gratefully acknowledged for their assistance in the FP assay. Special thanks to Silke Bauer for helpful discussions.

Appendix A. Supplementary material

Supplementary material related to this article can be found at http://dx.doi.org..... .

References

[1] V. Perrin, N. Dufour, C. Raoul, R. Hassig, E. Brouillet, P. Aebischer, R. Luthi-Carter, N. Deglon, Implication of the JNK pathway in a rat model of Huntington's disease, Exp. Neurol., 215 (2009) 191-200.

[2] L. Resnick, M. Fennell, Targeting JNK3 for the treatment of neurodegenerative disorders, Drug Discov. Today, 9 (2004) 932-939.

[3] S. Kumar, S.M. Blake, J.G. Emery, Intracellular signaling pathways as a target for the treatment of rheumatoid arthritis, Curr. Opin. Pharmacol., 1 (2001) 307-313.

[4] Y.J. Feng, Y.Y. Li, The role of p38 mitogen-activated protein kinase in the pathogenesis of inflammatory bowel disease, J. Dig. Dis., 12 (2011) 327-332.

[5] A. Mavropoulos, E.I. Rigopoulou, C. Liaskos, D.P. Bogdanos, L.I. Sakkas, The role of p38 MAPK in the aetiopathogenesis of psoriasis and psoriatic arthritis, Clin. Dev. Immunol., 2013 (2013) 569751.

[6] J.C. Betts, R.J. Mayer, R. Tal-Singer, L. Warnock, C. Clayton, S. Bates, B.E. Hoffman, C. Larminie, D. Singh, Gene expression changes caused by the p38 MAPK inhibitor dilmapimod in COPD patients: analysis of blood and sputum samples from a randomized, placebo-controlled clinical trial, Pharmacol. Res. Perspect., 3 (2015) e00094.

[7] W. MacNee, R.J. Allan, I. Jones, M.C. De Salvo, L.F. Tan, Efficacy and safety of the oral p38 inhibitor PH-797804 in chronic obstructive pulmonary disease: a randomised clinical trial, Thorax, 68 (2013) 738-745.

[8] S.A. Correa, K.L. Eales, The Role of p38 MAPK and Its Substrates in Neuronal Plasticity and Neurodegenerative Disease, J. Signal Transduct., 2012 (2012) 649079.

[9] D.N. Krementsov, T.M. Thornton, C. Teuscher, M. Rincon, The emerging role of p38 mitogen-activated protein kinase in multiple sclerosis and its models, Mol. Cell. Biol., 33 (2013) 3728-3734.

[10] L. Munoz, A.J. Ammit, Targeting p38 MAPK pathway for the treatment of Alzheimer's disease, Neuropharmacology, 58 (2010) 561-568.

[11] P. Koch, M. Gehringer, S.A. Laufer, Inhibitors of c-Jun N-terminal kinases: an update, J. Med. Chem., 58 (2015) 72-95.

[12] M. Gehringer, F. Muth, P. Koch, S.A. Laufer, c-Jun N-terminal kinase inhibitors: a patent review (2010-2014), Expert Opin. Ther. Pat., 25 (2015) 849-872.

[13] S. Bühler, S.A. Laufer, P38 MAPK inhibitors: a patent review (2012-2013), Expert Opin. Ther. Pat., 24 (2014) 535-554.

[14] A.M. Manning, R.J. Davis, Targeting JNK for therapeutic benefit: from junk to gold?, Nat. Rev. Drug Discov., 2 (2003) 554-565.

[15] A. Cuenda, S. Rousseau, p38 MAP-kinases pathway regulation, function and role in human diseases, Biochim. Biophys. Acta, 1773 (2007) 1358-1375.

[16] B. Kaminska, MAPK signalling pathways as molecular targets for anti-inflammatory therapy--from molecular mechanisms to therapeutic benefits, Biochim. Biophys. Acta, 1754 (2005) 253-262.

[17] S. Kumar, J. Boehm, J.C. Lee, p38 MAP kinases: key signalling molecules as therapeutic targets for inflammatory diseases, Nat. Rev. Drug Discov., 2 (2003) 717-726.

[18] R.J. Davis, Signal transduction by the JNK group of MAP kinases, Cell, 103 (2000) 239-252.

[19] Y. Liu, N.S. Gray, Rational design of inhibitors that bind to inactive kinase conformations, Nat. Chem. Biol., 2 (2006) 358-364.

[20] J.E. Sullivan, G.A. Holdgate, D. Campbell, D. Timms, S. Gerhardt, J. Breed, A.L. Breeze, A. Bermingham, R.A. Pauptit, R.A. Norman, K.J. Embrey, J. Read, W.S. VanScyoc, W.H.J. Ward, Prevention of MKK6-dependent activation by binding to p38 alpha MAP kinase, Biochemistry, 44 (2005) 16475-16490.

[21] F. Filomia, F. De Rienzo, M.C. Menziani, Insights into MAPK p38alpha DFG flip mechanism by accelerated molecular dynamics, Bioorg. Med. Chem., 18 (2010) 6805-6812.

[22] Z. Zhao, H. Wu, L. Wang, Y. Liu, S. Knapp, Q. Liu, N.S. Gray, Exploration of type II binding mode: A privileged approach for kinase inhibitor focused drug discovery?, ACS Chem. Biol., 9 (2014) 1230-1241.

[23] A. Backes, B. Zech, B. Felber, B. Klebl, G. Müller, Small-molecule inhibitors binding to protein kinases. Part I: exceptions from the traditional pharmacophore approach of type I inhibition, Expert Opin. Drug Discov., 3 (2008) 1409-1425.

[24] M. Vogtherr, K. Saxena, S. Hoelder, S. Grimme, M. Betz, U. Schieborr, B. Pescatore, M. Robin, L. Delarbre, T. Langer, K.U. Wendt, H. Schwalbe, NMR characterization of kinase p38 dynamics in free and ligand-bound forms, Angew. Chem., Int. Ed., 45 (2006) 993-997.

[25] A. Backes, B. Zech, B. Felber, B. Klebl, G. Müller, Small-molecule inhibitors binding to protein kinase. Part II: the novel pharmacophore approach of type II and type III inhibition, Expert Opin. Drug Discov., 3 (2008) 1427-1449.

[26] C. Pargellis, L. Tong, L. Churchill, P.F. Cirillo, T. Gilmore, A.G. Graham, P.M. Grob, E.R. Hickey, N. Moss, S. Pav, J. Regan, Inhibition of p38 MAP kinase by utilizing a novel allosteric binding site, Nat. Struct. Biol., 9 (2002) 268-272.

[27] M. Goettert, S. Luik, R. Graeser, S.A. Laufer, A direct ELISA assay for quantitative determination of the inhibitory potency of small molecules inhibitors for JNK3, J. Pharm. Biomed. Anal., 55 (2011) 236-240.

[28] M. Goettert, R. Graeser, S.A. Laufer, Optimization of a nonradioactive immunosorbent assay for p38alpha mitogen-activated protein kinase activity, Anal. Biochem., 406 (2010) 233-234.

[29] J.R. Simard, M. Getlik, C. Grutter, V. Pawar, S. Wulfert, M. Rabiller, D. Rauh, Development of a fluorescent-tagged kinase assay system for the detection and characterization of allosteric kinase inhibitors, J. Am. Chem. Soc., 131 (2009) 13286-13296.

[30] H. Tecle, F. Feru, H. Liu, C. Kuhn, G. Rennie, M. Morris, J. Shao, A.C. Cheng, D. Gikunju, J. Miret, R. Coli, S.H. Xi, S.L. Clugston, S. Low, S. Kazmirski, Y.H. Ding, Q. Cao, T.L. Johnson, G.D. Deshmukh, J.P. DiNitto, J.C. Wu, J.M. English, The design, synthesis and potential utility of fluorescence probes that target DFG-out conformation of p38alpha for high throughput screening binding assay, Chem. Biol. Drug Des., 74 (2009) 547-559.

[31] T.J. Burke, K.R. Loniello, J.A. Beebe, K.M. Ervin, Development and application of fluorescence polarization assays in drug discovery, Comb. Chem. High Throughput Screen., 6 (2003) 183-194.

[32] D.M. Jameson, J.C. Croney, Fluorescence polarization: past, present and future, Comb. Chem. High Throughput Screen., 6 (2003) 167-173.

[33] S.M. Vogel, M.R. Bauer, A.C. Joerger, R. Wilcken, T. Brandt, D.B. Veprintsev, T.J. Rutherford, A.R. Fersht, F.M. Boeckler, Lithocholic acid is an endogenous inhibitor of MDM4 and MDM2, Proc. Natl. Acad. Sci. U. S. A., 109 (2012) 16906-16910.

[34] J.R. Lakowicz, Principles of Fluorescence Spectroscopy, Springer, 2006, pp. 353-380.

[35] A.M. Rossi, C.W. Taylor, Analysis of protein-ligand interactions by fluorescence polarization, Nat. Protoc., 6 (2011) 365-387.

[36] A. Lange, M. Günther, F. Michael Büttner, M.O. Zimmermann, J. Heidrich, S. Hennig, S. Zahn, C. Schall, A. Sievers-Engler, F. Ansideri, P. Koch, M. Laemmerhofer, T. Stehle, S.A. Laufer, F.M. Boeckler, Targeting the Gatekeeper MET146 of C-Jun N-Terminal Kinase 3 Induces a Bivalent Halogen/Chalcogen Bond, J. Am. Chem. Soc., 137 (2015) 14640-14652.

[37] L. Munoz, R. Selig, Y.T. Yeung, C. Peifer, D. Hauser, S. Laufer, Fluorescence polarization binding assay to develop inhibitors of inactive p38alpha mitogen-activated protein kinase, Anal. Biochem., 401 (2010) 125-133.

[38] C.E. Fitzgerald, S.B. Patel, J.W. Becker, P.M. Cameron, D. Zaller, V.B. Pikounis, S.J. O'Keefe, G. Scapin, Structural basis for p38alpha MAP kinase quinazolinone and pyridol-pyrimidine inhibitor specificity, Nat. Struct. Biol., 10 (2003) 764-769.

[39] T. Kamenecka, J. Habel, D. Duckett, W. Chen, Y.Y. Ling, B. Frackowiak, R. Jiang, Y. Shin, X. Song, P. LoGrasso, Structure-activity relationships and X-ray structures describing the selectivity of aminopyrazole inhibitors for c-Jun N-terminal kinase 3 (JNK3) over p38, J. Biol. Chem., 284 (2009) 12853-12861.

[40] H.M. Berman, J. Westbrook, Z. Feng, G. Gilliland, T.N. Bhat, H. Weissig, I.N. Shindyalov, P.E. Bourne, The Protein Data Bank, Nucleic Acids Res., 28 (2000) 235-242.

[41] O. Korb, T. Stutzle, T.E. Exner, Empirical Scoring Functions for Advanced Protein-Ligand Docking with PLANTS, J. Chem. Inf. Model., 49 (2009) 84-96.

[42] G. Jones, P. Willett, R.C. Glen, A.R. Leach, R. Taylor, Development and validation of a genetic algorithm for flexible docking, J. Mol. Biol., 267 (1997) 727-748.

[43] M.D. Eldridge, C.W. Murray, T.R. Auton, G.V. Paolini, R.P. Mee, Empirical scoring functions .1. The development of a fast empirical scoring function to estimate the binding affinity of ligands in receptor complexes, J. Comput. Aided Mol. Des., 11 (1997) 425-445.

[44] L. Revesz, E. Blum, F.E. Di Padova, T. Buhl, R. Feifel, H. Gram, P. Hiestand, U. Manning, G. Rucklin, Novel p38 inhibitors with potent oral efficacy in several models of rheumatoid arthritis, Bioorg. Med. Chem. Lett., 14 (2004) 3595-3599.

[45] Z. Nikolovska-Coleska, R. Wang, X. Fang, H. Pan, Y. Tomita, P. Li, P.P. Roller, K. Krajewski, N.G. Saito, J.A. Stuckey, S. Wang, Development and optimization of a binding assay for the XIAP BIR3 domain using fluorescence polarization, Anal. Biochem., 332 (2004) 261-273.

[46] R.N.-C. Wang, Z.; Fang, X.; Wang, S., From IC50 to Ki: A General Mathematical Solution for Fluorescence-Based Competitive Binding Assays, unpublished results.

[47] P.W. Iversen, B. Beck, Y.F. Chen, W. Dere, V. Devanarayan, B.J. Eastwood, M.W. Farmen, S.J. Iturria, C. Montrose, R.A. Moore, J.R. Weidner, G.S. Sittampalam, HTS Assay Validation, in: G.S. Sittampalam, N.P. Coussens, H. Nelson, M. Arkin, D. Auld, C. Austin, B. Bejcek, M. Glicksman, J. Inglese, P.W. Iversen, Z. Li, J. McGee, O. McManus, L. Minor, A. Napper, J.M. Peltier, T. Riss, O.J. Trask, Jr., J. Weidner (Eds.) Assay Guidance Manual, Bethesda (MD), 2004.

[48] G. Scapin, S.B. Patel, J. Lisnock, J.W. Becker, P.V. LoGrasso, The structure of JNK3 in complex with small molecule inhibitors: Structural basis for potency and selectivity, Chem. Biol., 10 (2003) 705-712.

[49] Z.L. Wang, B.J. Canagarajah, J.C. Boehm, S. Kassisa, M.H. Cobb, P.R. Young, S. Abdel-Meguid, J.L. Adams, E.J. Goldsmith, Structural basis of inhibitor selectivity in MAP kinases, Struct. Fold Des., 6 (1998) 1117-1128.

[50] S.A. Laufer, A.J. Liedtke, A concise and optimized four-step approach toward 2-(aryl-)alkylsulfanyl-, 4(5)-aryl-, 5(4)-heteroaryl-substituted imidazoles using alkyl- or arylalkyl thiocyanates, Tetrahedron Lett., 47 (2006) 7199-7203.

[51] P. Koch, H. Jahns, V. Schattel, M. Goettert, S. Laufer, Pyridinylquinoxalines and pyridinylpyridopyrazines as lead compounds for novel p38 alpha mitogen-activated protein kinase inhibitors, J. Med. Chem., 53 (2010) 1128-1137.

[52] B. Radzisewski, Über Glyoxalin und seine Homologe, Ber. Dtsch. Chem. Ges., 15 (1882) 2706-2708.

[53] W.A. Lea, A. Simeonov, Fluorescence polarization assays in small molecule screening, Expert Opin. Drug Discov., 6 (2011) 17-32.

[54] N.J. Moerke, Fluorescence Polarization (FP) Assays for Monitoring Peptide-Protein or Nucleic Acid-Protein Binding, Curr. Protoc. Chem. Biol., 1 (2009) 1-15.

[55] A. El-Gokha, S.A. Laufer, P. Koch, An optimized and versatile synthesis to pyridinylimidazole-type p38alpha mitogen activated protein kinase inhibitors, Org. Biomol. Chem., 13 (2015) 10699-10704.

[56] P. Koch, C. Bäuerlein, H. Jank, S. Laufer, Targeting the ribose and phosphate binding site of p38 mitogen-activated protein (MAP) kinase: Synthesis and biological testing of 2-alkylsulfanyl-, 4(5)-aryl-, 5(4)-heteroaryl-substituted imidazoles, J. Med. Chem., 51 (2008) 5630-5640.

[57] B.L. Bennett, D.T. Sasaki, B.W. Murray, E.C. O'Leary, S.T. Sakata, W. Xu, J.C. Leisten, A. Motiwala, S. Pierce, Y. Satoh, S.S. Bhagwat, A.M. Manning, D.W. Anderson, SP600125, an anthrapyrazolone inhibitor of Jun N-terminal kinase, Proc. Natl. Acad. Sci. U. S. A., 98 (2001) 13681-13686.

[58] P. Gaillard, I. Jeanclaude-Etter, V. Ardissone, S. Arkinstall, Y. Cambet, M. Camps, C. Chabert, D. Church, R. Cirillo, D. Gretener, S. Halazy, A. Nichols, C. Szyndralewiez, P.A. Vitte, J.P. Gotteland, Design and synthesis of the first generation of novel potent, selective, and in vivo active (benzothiazol-2-yl)acetonitrile inhibitors of the c-Jun N-terminal kinase, J. Med. Chem., 48 (2005) 4596-4607.

[59] S.C. Koeberle, J. Romir, S. Fischer, A. Koeberle, V. Schattel, W. Albrecht, C. Grutter, O. Werz, D. Rauh, T. Stehle, S.A. Laufer, Skepinone-L is a selective p38 mitogen-activated protein kinase inhibitor, Nat. Chem. Biol., 8 (2012) 141-143.

[60] L.J. Adams, J.C. Boehm, C. Jeffrey, R. Hall, Q. Jin, J. Kasparec, D.J. Silva, J.J. Taggart, Novel compounds, WO/2002/059083 A2, 2001.

[61] S.A. Laufer, D.R. Hauser, D.M. Domeyer, K. Kinkel, A.J. Liedtke, Design, synthesis, and biological evaluation of novel Tri- and tetrasubstituted imidazoles as highly potent and specific ATP-mimetic inhibitors of p38 MAP kinase: focus on optimized interactions with the enzyme's surface-exposed front region, J. Med. Chem., 51 (2008) 4122-4149.

[62] S. Fischer, H.K. Wentsch, S.C. Mayer-Wrangowski, M. Zimmermann, S.M. Bauer, K. Storch, R. Niess, S.C. Koeberle, C. Grutter, F.M. Boeckler, D. Rauh, S.A. Laufer, Dibenzosuberones as p38 mitogen-activated protein kinase inhibitors with low ATP competitiveness and outstanding whole blood activity, J. Med. Chem., 56 (2013) 241-253.

Highlights

- Two novel probes binding both active and inactive JNK3 and p38α MAPK were synthesized.
- First reported example of FP-based binding assay for JNK3.
- FP-based competition binding assays were developed and optimized.
- Both FP binding assays showed correlation with ELISA activity assay.
- The assays presented proved to be suitable for HTS format.